‘Galileo Galilei’ (GG): space test of the weak equivalence principle to 10^{-17} and laboratory demonstrations

2012 Class. Quantum Grav. 29 184011

(http://iopscience.iop.org/0264-9381/29/18/184011)

Class. Quantum Grav. **29** (2012) 184011 (18pp) doi:10.1088/0264-9381/29/18/184011

'Galileo Galilei' (GG): space test of the weak equivalence principle to 10^{-17} and laboratory demonstrations

A M Nobili[1,2], M Shao[3], R Pegna[2], G Zavattini[4,5], S G Turyshev[3], D M Lucchesi[2,6], A De Michele[1], S Doravari[7], G L Comandi[2], T R Saravanan[1], F Palmonari[8,9], G Catastini[10] and A Anselmi[10]

[1] Department of Physics 'E Fermi', University of Pisa, Largo Bruno Pontecorvo 3, 56127 Pisa, Italy
[2] INFN-Istituto Nazionale di Fisica Nucleare, Sezione di Pisa, Largo Bruno Pontecorvo 3, 56127 Pisa, Italy
[3] Jet Propulsion Laboratory, California Institute of Technology, 4800 Oak Grove Drive, Pasadena, CA 91109, USA
[4] Department of Physics, University of Ferrara, Via Saragat 1, 44122 Ferrara, Italy
[5] INFN-Istituto Nazionale di Fisica Nucleare, Sezione di Ferrara, Via Saragat 1, 44122 Ferrara, Italy
[6] INAF-IAPS-Istituto di Astrofisica e Planetologia Spaziali, Via Fosso del Cavaliere 100, 00133 Rome, Italy
[7] LIGO Laboratory California Institute of Technology, Pasadena, CA 91125, USA
[8] Department of Physics, University of Bologna, Viale Berti Pichat 6/2 40127 Bologna, Italy
[9] INFN-Istituto Nazionale di Fisica Nucleare, Sezione di Bologna, Viale Berti Pichat 6/2 40127 Bologna, Italy
[10] Thales Alenia Space Italia, Strada Antica di Collegno 253, 10146 Torino, Italy

E-mail: nobili@dm.unipi.it

Received 23 February 2012, in final form 23 July 2012
Published 15 August 2012
Online at stacks.iop.org/CQG/29/184011

Abstract

The small satellite 'Galileo Galilei' (GG) will test the universality of free fall and hence the weak equivalence principle which is the founding pillar of general relativity to 1 part in 10^{17}. It will use proof masses whose atoms differ substantially from one another in their mass energy content, so as to maximize the chance of violation. GG will improve by four orders of magnitude the current best 'Eöt-Wash' tests based on slowly rotating torsion balances, which have been able to reach their thermal noise level. In GG, the expected violation signal is a relative displacement between the proof masses of $\simeq 0.6$ pm caused by a differential acceleration $a_{\rm GG} \simeq 8 \times 10^{-17}\,{\rm ms}^{-2}$ pointing to the center of mass of the Earth as the satellite orbits around it at $\nu_{\rm GG} \simeq 1.7 \times 10^{-4}$ Hz. GG will fly an innovative acceleration sensor based on rapidly rotating macroscopic test masses weakly coupled in 2D which up-converts the signal to $\nu_{\rm spin} \simeq 1$ Hz, a value well above the frequency of natural oscillations of the masses relative to each other $\nu_d = 1/T_d \simeq 1/(540\,{\rm s})$. The sensor is unique in that it ensures high rotation frequency, low thermal noise and no attenuation of the signal strength (Pegna *et al* 2011 *Phys. Rev. Lett.* **107** 200801). A readout based on a very

low noise laser interferometry gauge developed at Jet Propulsion Laboratory ($\simeq$ 1 pm $\mathrm{Hz}^{-1/2}$ at 1 Hz demonstrated) allows the short integration time to be fully exploited. A full scale sensor with the same degrees of freedom and the same dynamical features as the one to fly in GG has been setup on ground (GGG). The proof masses of GGG are affected by acceleration and tilt noise acting on the rotating shaft because of ball bearings and terrain microseismicity (both absent in space). Overall, by means of appropriate 2D flexure joints, these noise sources have been reduced by a factor almost 10^5 down to a differential acceleration between the proof masses of $\simeq 7 \times 10^{-11}\,\mathrm{m\,s^{-2}}$ (at 1.7×10^{-4} Hz up-converted by rotation to $\simeq$ 0.2 Hz). The corresponding noise in the relative displacements of the proof masses, read by co-rotating capacitance bridges, is $\simeq$ 180 pm, which is 300 times larger than the target in space. GGG error budget shows that it can reach a differential acceleration sensitivity $a_{\mathrm{GGGgoal}} \simeq 8 \times 10^{-16}\,\mathrm{m\,s^{-2}}$, not limited by thermal noise. This value is only a factor 10 larger than what GG must reach in space to meet its target, and slightly smaller than the acceleration noise of the torsion balance. It can be achieved partly by means of weaker joints and an optimized mechanical design—so as to improve the attenuation factor—and partly by replacing the current ball bearings with much less noisy air bearings (also used in torsion balance tests) so as to reduce input noise. A laser gauge readout with noise level $r_{\mathrm{laser\text{-}ro}} \simeq 30\,\mathrm{pm\,Hz^{-1/2}}$ at $0.2 \div 3$ Hz will be implemented.

PACS numbers: 04.80.Cc, 07.87.+v

(Some figures may appear in colour only in the online journal)

1. Why test the weak equivalence principle in space?

General relativity (GR) is the best theory of gravity to date. It governs physics at the macroscopic and cosmic scales and it has been highly successful. However, all attempts at merging gravity with the other forces of nature have failed and most of the mass of the universe is unexplained. GR is based on the hypothesis that the gravitational force is composition independent: in a gravitational field all bodies fall with the same acceleration regardless of their mass and composition. This property is unique to gravity. It is referred to as the universality of free fall, and it is the direct consequence of the equivalence between inertial and gravitational masses assumed by Newton in 1687 in the opening paragraph of the *Principia*. It is the basic assumption of the much more general equivalence principle formulated by Einstein [2], which 8 years later led him to GR. This principle is known as the strong equivalence principle (see Dicke's formulation [3, p 4]) or as Einstein's equivalence principle [4] while Newton's equivalence of inertial and gravitational masses is now referred to as the weak equivalence principle (WEP).

If the universality of free fall and the WEP are invalidated by experiments, so is the strong equivalence principle. As a result, either GR should be amended or we are in the presence of a new force of nature.

Tests of WEP are unique tests of GR. They address the assumed composition independence of gravity which sets it aside from all other forces of nature; moreover, if properly designed, they are *null experiments* and therefore can reach very high sensitivity. For these reasons, they are the most deeply probing tests in the search for new physics beyond GR and the

current *impasse* and should therefore be pushed to higher and higher sensitivity whenever the experimental possibility for an improvement arises.

Such improvements occurred several times in history. In 1600, Galileo suspended masses made up of different materials by wires rather than dropping them from a height (to avoid limitations due to the short time of fall and the bodies release errors) and found that they fall with the same acceleration with a fractional difference of $\simeq 10^{-3}$ [5, 6]. In the early 1900, Eötvös coupled the proof masses by placing them on a torsion balance whose high sensitivity and perfect rejection of common-mode effects allowed him to reach the amazing level of 10^{-8} [7] on which Einstein relied [8, p 114] . In the field of the Earth, the signal is DC and the torsion balance test lacks modulation. In order to overcome this limitation without rotating the balance, Dicke and Braginsky in the 1960s and 1970s searched for violation in the field of the Sun exploiting the diurnal rotation of the Earth in order to modulate the signal. Although the signal from the Sun is slightly weaker than that from the Earth, signal modulation allowed them to make a very substantial improvement reaching 10^{-11} [9] and 10^{-12} [10]. In the last two decades, the Eöt-Wash group has managed to rotate the balance itself about 70 times faster than the Earth's rotation. They have confirmed no violation to 10^{-12} [11] in the field of the Sun and reached 10^{-13} [12] in the field of the Earth. For the Earth and the Moon in the field of the Sun, lunar laser ranging (LLR) has found no violation at the level 10^{-13} [13, 14].

Rotating torsion balances have been pushed to their thermal noise limit [15, figure 20]. The LLR community is improving laser ranging technology and physical modeling [16], but there are fundamental limitations [17]. In both cases, one order of magnitude gain may be possible but a significant improvement is out of reach.

As for tests based on dropping cold atoms, they are at the level of 10^{-7}, many orders of magnitude less sensitive than it has been achieved with macroscopic bodies. They have yet to match the best result $\Delta g/g \simeq 3 \times 10^{-9}$ obtained in measuring the local gravitational acceleration by dropping a single species of atoms [18]. More importantly, they reach this sensitivity dropping two isotopes of the same atom which differ by two neutrons only [19]. In this case, the difference in the mass energy content is so small that violation is very unlikely to occur anyway, which makes the scientific relevance of the test rather limited.

A radically new type of experiment is necessary to improve the current experimental limit by several orders of magnitude thus deeply probing this so far unexplored domain of physics. Such a noticeable improvement appears to be possible with a torsion balance type of experiment in which two weakly coupled macroscopic proof masses orbit the Earth inside a low altitude spacecraft ($h \simeq 600$ km). The experiment combines the strong signal of mass dropping tests without their disadvantages. As in mass dropping tests, the signal is strong: $g(h) \simeq 8\,\mathrm{m\,s^{-2}}$, exceeds by about three orders of magnitude the driving acceleration on the test masses of the balance on ground. Yet, while mass release errors are the limiting error source in mass dropping experiments, in a balance-type experiment they are not an issue because the test masses are coupled. In addition, the short duration of mass dropping experiments is overcome because in orbit it is as if the proof masses were falling from an 'infinitely' tall tower; the experiment lasts as long as the mission lasts.

The absence of weight allows extremely weak suspensions to be used with a sensitivity close to that of a good quality torsion fiber. Isolation of the laboratory (the spacecraft) is a great additional advantage. Overall, an improvement by four orders of magnitude is within reach.

2. How can GG improve WEP tests by four orders of magnitude at room temperature?

The Eöt-Wash group has found no violation of WEP in the field of the Earth to 10^{-13}, with an acceleration noise (1σ) $1.8 \times 10^{-15}\,\mathrm{m\,s^{-2}}$ obtained from a 75 d data set [12]. They have reached

the level of thermal noise from internal damping in the suspension fiber competing with the signal up-converted at the rotation frequency of the balance, and this is the experiment limiting factor (see [15, figure 20]). GG aims at $\eta_{\rm GG} = 10^{-17}$ orbiting at 600 km altitude around the Earth, where $g(h) \simeq 8\,{\rm m\,s^{-2}}$. It must therefore detect a differential acceleration between the test masses $a_{\rm GG} \simeq 8 \times 10^{-17}\,{\rm m\,s^{-2}}$. This is 23 times smaller than the acceleration noise of the Eöt-Wash torsion balance. μSCOPE [20] aims at $\eta_{\mu{\rm scope}} = 10^{-15}$ at a similar altitude and must detect a 100 times bigger acceleration $a_{\mu{\rm scope}} \simeq 8 \times 10^{-15}\,{\rm m\,s^{-2}}$ which is also 4.4 times larger than the torsion balance acceleration noise. For both GG and μSCOPE, the signal (in the inertial J2000 equatorial reference frame) is at the satellite orbital frequency $\nu_{\rm GG} \simeq 1.7 \times 10^{-4}\,{\rm Hz}$.

All these experiments are at room temperature and exploit rotation of the sensor in order to up-convert the signal to higher frequency. On ground, the signal is DC (in the North–South direction) and the torsion balance rotates around the vertical axis with a period of 1200 s up-converting the signal to $\nu_{\rm sTB} \simeq 8.4 \times 10^{-4}\,{\rm Hz}$. μSCOPE rotates so as to up-convert the signal to $\nu_{\mu{\rm scope}} \simeq 8 \times 10^{-4}\,{\rm Hz}$ [20]. GG rotates at $\nu_{\rm spin} \simeq 1\,{\rm Hz}$ up-converting the signal to $\nu_{\rm spin} \pm \nu_{\rm GG} \simeq \nu_{\rm spin} \simeq 1\,{\rm Hz}$.

As shown in [21], thermal noise from internal (or structural) damping decreases with increasing frequency as $1/\sqrt{f}$. The measured noise of the Eöt-Wash torsion balance matches well the behavior predicted in [21]. This is reported in [15, figure 20] where in a log–log plot the predicted thermal noise is a straight line. Note that, as the authors stress, at higher frequencies readout noise dominates, and therefore, the $1/\sqrt{f}$ behavior of the measured noise is lost.

In [1], it has been demonstrated how the $1/\sqrt{f}$ dependence of structural thermal noise affects a 2D mechanical oscillator rotating above its natural (resonance) frequency like GG. We therefore quantitatively compare in figure 1 the GG and μSCOPE thermal noise (μSCOPE is a 1D rotating oscillator similar to the torsion balance in this respect) on the basis of the signal modulation frequency only.

According to the principal investigator [20], μSCOPE is expected to be limited by thermal noise due internal damping in the gold wire of 5 μm diameter and 2.5 cm length which connects the test masses to the instrument cages. At the signal frequency $\nu_{\mu{\rm scope}} \simeq 8 \times 10^{-4}\,{\rm Hz}$, it is estimated to amount to $1.4 \times 10^{-12}\,{\rm m\,s^{-2}Hz^{-1/2}}$ [20, table 5]. With the target $\eta_{\mu{\rm scope}} = 10^{-15}$ and for a signal-to-noise ratio SNR = 2, the required integration time is $t_{{\rm int}-\mu{\rm scope}} \simeq 1.23 \times 10^5\,{\rm s} = 1.4\,{\rm d}$, i.e. the mission goal can be reached in 20.8 orbits of the satellite (as stated also in [22, p 16]). Should μSCOPE aim at 10^{-17} like GG it would require a 10^4 times longer integration time (about 39 years) which is obviously unfeasible.

For GG, the thermal noise force per unit of reduced mass competing with the signal after an integration time $t_{\rm int}$ is given in [1] and reads

$$a_{\rm th} \simeq \sqrt{\frac{4K_BT\omega_d^2\phi(\omega_{\rm spin})}{\mu\omega_{\rm spin}}}\,\frac{1}{\sqrt{t_{\rm int}}}, \tag{1}$$

where $T \simeq 300\,{\rm K}$ is the equilibrium temperature; $K_B = 1.38 \times 10^{-23}\,{\rm J\,K^{-1}}$ is the Boltzmann constant and (for GG) $\omega_{\rm spin} \simeq 2\pi\,{\rm rad\,s^{-1}}$ is the spin angular frequency; $\mu = m/2 = 5\,{\rm kg}$ is the reduced mass of the oscillator ($m = 10\,{\rm kg}$ is the mass of each test cylinder); $\omega_d \simeq 2\pi/540\,{\rm rad\,s^{-1}}$ is the natural differential frequency; $\phi(\omega_{\rm spin}) \simeq 1/20\,000$ is the loss angle due to internal losses in the proof masses suspensions at the spin frequency. Large test masses are chosen in order to reduce thermal noise and in consideration of the fact that rotation makes the effects of mass anomalies DC, while it up-converts the signal to the (high) spin frequency. U-shape laminar suspensions will be manufactured of CuBe because this alloy, if properly treated, is known to have a good mechanical quality. A natural differential period

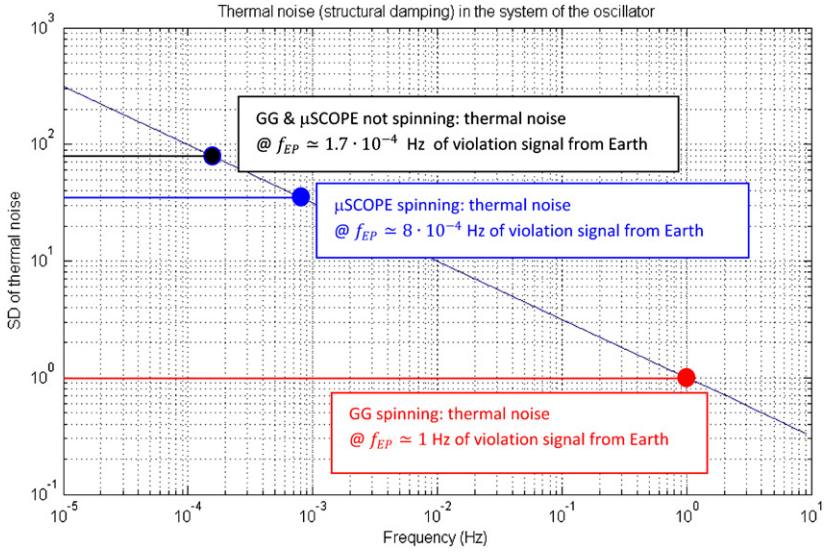

Figure 1. The inclined line shows—in arbitrary units—the linear spectral density (SD) of the structural (internal) damping thermal noise as a function of frequency, measured in the system in which the suspensions are at rest. The expected $1/\sqrt{f}$ behavior [21] has been confirmed experimentally by the rotating torsion balances (see figure 20 in [15] where the predicted $1/\sqrt{f}$ behavior is also shown as a black straight line). If they were not spinning, GG and μSCOPE would be affected by a violation of UFF/WEP in the field of the Earth at their orbital frequency $\simeq 1.7 \times 10^{-4}$ Hz. As far as the frequency dependence of internal damping is concerned, their thermal noise would be the same, and it is depicted by the black bullet. However, once they are set in rotation, μSCOPE (1D sensor) up-converts the expected signal to $\nu_{\mu\text{scope}} \simeq 8 \times 10^{-4}$ Hz while GG (2D sensor) up-converts it to $\nu_{\text{spin}} \simeq 1$ Hz. On the internal damping straight line, the corresponding thermal noise is represented by the blue and the red bullet, respectively. The advantage of a higher rotation frequency is apparent: it makes the linear SD of GG thermal noise a factor $\sqrt{\nu_{\mu\text{scope}}/\nu_{\text{spin}}} \simeq 35.4$ times smaller than that of μSCOPE. At a given frequency of the signal, thermal noise competing with it is a random noise, and therefore, it decreases as the square root of the integration time. We conclude that, because of rotation only, the integration time required for GG to reduce thermal noise below a target signal is a factor $\nu_{\mu\text{scope}}/\nu_{\text{spin}} \simeq 1250$ shorter than the integration time needed for μSCOPEto do the same.

of 540 s can be obtained with U-shape CuBe flexures that can be manufactured, tested and launched safely ($\omega_d = \sqrt{k/\mu}$, with k being the elastic coupling constant of the proof masses in each direction of the sensitive plane). A rotation frequency of 1 Hz is a standard rotation frequency for spin stabilized spacecraft. Near this frequency, loss angles close to 1/20 000 have been measured [23, 24].

Note that formulas similar to (1) are used to calculate the thermal noise of the rotating torsion balance [15] as well as of μSCOPE[20]. For GG, with the target $\eta_{\text{GG}} = 10^{-17}$ and SNR $= 2$, the required integration time is only about 1 h. Taking into account also thermal noise due to residual gas damping and to eddy currents, we find that a total integration time of about 3 h is needed, with 10^{-5} Pa residual pressure, 2 cm gap and reduction by a factor 100 of the magnetic field of the Earth to be provided by a μ-metal shield [25]. It is planned that a full test to $\eta_{\text{GG}} = 10^{-17}$ will be performed with 1 d measurement data. Thus, all the available time (in a total 9 month mission duration) can be devoted to checking for systematic errors under varying dynamical conditions—provided naturally by the spin axis of the satellite being fixed in space (by conservation laws), while the orbit plane obeys the $\simeq 1^{\text{o}}$/d regression of

the nodes of sun-synchronous orbits—which will allow the expected violation signal to be separated beyond question, with one accelerometer only, from competing effects of classical physics due to their different known signature [26].

Scientists agree on the advantages of up-converting a low frequency (or DC) signal to higher frequency (the higher the better) by rotating the oscillator used to measure it. However, modulation by rapid rotation is known to face two major problems. The primary one is that in the case of 1D mechanical oscillators the effect of a force up-converted above the natural frequency of the oscillator is reduced as the ratio *natural-to-signal frequency squared*. Precisely for this reason, 1D oscillators are used to suspend the mirrors of the VIRGO gravitational wave laser interferometer detector where the purpose is to reduce the effects of microseismic terrain noise at frequencies higher than the resonance frequency of the oscillator. Secondly, rotating macroscopic bodies are affected by unbalance effects which at a first glance are expected to be higher at higher rotation frequencies.

These problems are typical of 1D oscillators, but they disappear in 2D oscillators like GG in which two concentric coaxial cylinders are weakly coupled with elastic constant k in each direction of the plane perpendicular to the symmetry axis and rotate around it with the angular velocity $\omega_{\rm spin}$. The general solution of the equations of motion (in the inertial not in rotating reference frame) for the relative position vector $\vec{r}(t)$ of the test masses (with $\omega_{\rm spin}$ much higher than both the frequency of the force signal and the natural frequency of the system) is given by [1]

$$\vec{r}(t) \simeq -\vec{\epsilon}\left(\frac{\omega_d}{\omega_{\rm spin}}\right)^2 \begin{pmatrix}\cos(\omega_{\rm spin}t+\varphi)\\ \sin(\omega_{\rm spin}t+\varphi)\end{pmatrix} + \frac{\vec{F}}{k} - \phi(\omega_{\rm spin})\frac{\vec{\omega}_{\rm spin}}{\omega_{\rm spin}} \times \frac{\vec{F}}{k}$$
$$+ A_0\, \mathrm{e}^{\phi(\omega_{\rm spin})\omega_d t/2} \begin{pmatrix}\cos(\omega_d t+\varphi_A)\\ \sin(\omega_d t+\varphi_A)\end{pmatrix} + B_0 \mathrm{e}^{-\phi(\omega_{\rm spin})\omega_d t/2} \begin{pmatrix}\cos(-\omega_d t+\varphi_B)\\ \sin(-\omega_d t+\varphi_B)\end{pmatrix}, \qquad (2)$$

where $\vec{F}$ is the external (differential) force acting between the masses in the plane of the oscillator at very low frequency (we consider it DC) and $\vec{\epsilon}$ is the offset vector from the rotation axis due to inevitable construction errors. $\vec{\epsilon}$ is fixed on the rotating oscillator. A rotating mechanical system described by these equations is known in rotordynamics as being *in the supercritical regime* to indicate that the rotation speed is higher than the natural—or critical—one (the resonance). The solution (2) is approximate in that the terms depending on the loss angle squared have been neglected. Such terms are certainly negligible in the GG case. Equation (2) is simplified also because it does not take into account the actual three-dimensional shape of the proof masses as hollow cylinders. In that case conical modes of the symmetry axes appear. However, it is known from the general theory of supercritical rotors, and it has been confirmed in this specific case that conical modes are naturally damped and do not give rise to any instability (see [27, section 3.2] and [23, chapter 6]). We can therefore consider (2) as representative of the main features of the dynamical behavior of the real system.

If no external force is applied and there are no losses, i.e. the loss angle $\phi(\omega_{\rm spin})$ is zero, only the first term in (2) is nonzero. The solution is the equilibrium position fixed in the rotating frame at a distance from the rotation axis smaller than the original offset ϵ by the factor $(\omega_{\rm spin}/\omega_d)^2 = 2.9\times10^5$ in GG. This is the auto-centered equilibrium position, whereby it is apparent that—contrary to common intuition—the faster the spin (compared to the natural frequency), the better the masses auto-center on one another. If the offset error of the GG test masses is 20 μm—which is feasible—they will auto-center to 70 pm, thus reducing very effectively and with no need for an active control classical gravity gradient (tidal) effects. The minus sign is very important. It shows that the equilibrium position is located on the rotor

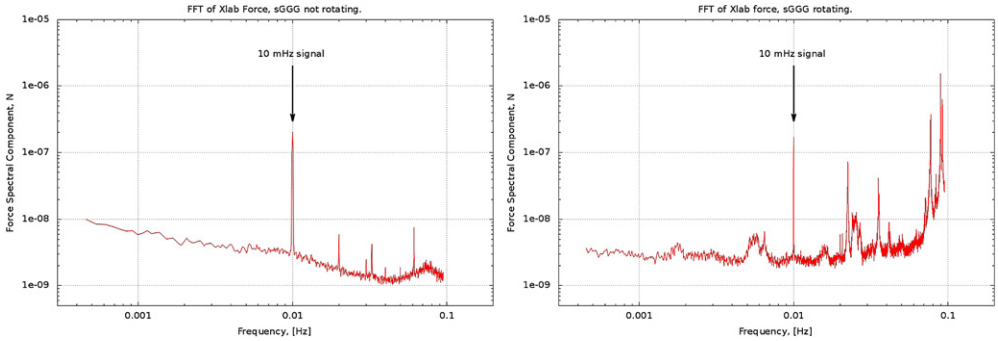

Figure 2. GGG measurements showing that in a 2D oscillator in supercritical rotation modulation of low-frequency signals by rotation at a frequency above resonance can be performed without the response of the oscillator being attenuated. (Left) GGG is not rotating and a differential force signal of about 2×10^{-7} N at 0.01 Hz is applied to the test cylinders along the $X_{\rm lab}$ direction of the horizontal plane of the lab. In this direction, the natural oscillation frequency of the test cylinders relative to each other is $\nu_x = 0.124$ Hz; thus, the force is applied below the resonance. (We add that the natural oscillation frequency in the perpendicular direction is $\nu_y = 0.063$ Hz). (Right) GGG has been set in rotation at $\nu_{\rm spin} = 0.19$ Hz, the natural oscillation frequency during rotation is $\nu_w = \sqrt{(\nu_x^2 + \nu_y^2)/2} = 0.098$ Hz and the same force signal is applied, in the same direction $X_{\rm lab}$. The force signal is up-converted by rotation above the GGG natural frequency. The experimental data have been demodulated back to the non-rotating horizontal plane of the lab for comparison with the non-rotating case shown before. If GGG were an oscillator in 1D, a similar rotation above its natural frequency would have attenuated its response to the signal by a factor 2.56, which would have been easily appreciated. We can see that in the non-rotating case (left plot) noise at lower frequencies is higher. The real advantage is to up-convert above resonance a signal at very low frequency, where noise in the absence of rotation is considerably higher. This is the case with GGG and GG. In the test presented here, the force was applied at a not so low frequency so that it could be performed with a short duration run. The purpose was to experimentally demonstrate that rotating a 2D oscillator does up-convert a signal to frequencies above resonance without reducing the response of the oscillator to the signal.

at the opposite direction of the original offset vector $\vec{\epsilon}$. Therefore, it can be reached only if motion is allowed in 2D [28, chapter 6].

If an external differential force $\vec{F}$ is applied (still with no losses), the second term of (2) is nonzero, while all the remaining ones are zero. The second term shows that the effect of the force is a differential displacement vector of the proof masses relative to each other, equal to $\vec{F}/k$ just as in the case in which the oscillator is not rotating. Therefore, even in the case in which the rotation of the oscillator up-converts the frequency of the applied force above the natural frequency of the oscillator (the resonance frequency), the effect of the force is still $\vec{F}/k$ thus showing that no attenuation occurs in the response of the oscillator. In the case of a 1D rotating oscillator with the same natural and rotation frequencies, the response to the same force would drop off as $(\omega_d/\omega_{\rm spin})^2$. If such attenuation were to occur in GG, the strength of the displacement signal when the system rotates would be a factor 2.9×10^5 smaller than it is at zero spin!

With the 'GG on Ground' (GGG) prototype (see section 4), which is a 2D oscillator like GG, we have experimentally demonstrated that the response to a low-frequency signal is indeed not attenuated when the oscillator rotates and up-converts it above the natural frequency. The result of this test is reported in figure 2 and described in the caption [31].

In the presence of losses, the response to the external force $\vec{F}$ shows a difference from the zero-spin case. That is given by the third term in (2). It represents a displacement

in the sensitive plane of the oscillator perpendicular to the applied force, but its size is smaller than the displacement in the direction of the force by a factor equal to the loss angle. The relevant losses are those at the spin frequency, which is another advantage of rapid rotation because losses are known to be smaller at higher frequencies than at lower ones (see e.g. [24]). In GG using CuBe joints with an appropriate manufacturing procedure and a loss angle $\simeq 1/20\,000$ at 1 Hz, the displacement perpendicular to the applied force is irrelevant.

In the general solution (2), the main effect of losses is expressed by the last two terms. They show that in the inertial reference frame the oscillator performs a combination of a forward and a backward orbital motion—known as *whirl motion*, with amplitudes and phases determined by initial conditions—at the (slow) natural frequency ω_d, and that the radii of such orbits are exponentially decaying in the case of the backward whirl and exponentially growing in the case of the forward one. Since the time constant is proportional to the (small) value of $\phi(\omega_{\rm spin})$, the exponentially growing whirl is a weak instability. In every natural/whirl period, the radius of the forward whirl grows by the fraction $\pi\phi(\omega_{\rm spin})$, and hence, the tangential force which produces the growth is—in modulus—$kr\phi(\omega_{\rm spin})$, which is a very small fraction of the elastic force, requiring a correspondingly small force to stabilize it. Its frequency is the natural one and does not interfere with the signal [30, 29]. In the GGG prototype, forward whirl motion is routinely controlled.

Small force experiments need very low ω_d for high sensitivity and very fast rotation in order to move the signal to a much higher frequency where thermal noise due to internal damping is much lower. This is the very definition of a rotor in the supercritical regime, which in turn is known to require two degrees of freedom. This shows why a 2D rotating oscillator suits UFF/WEP tests while one limited to 1D does not.

It should be noted for completeness that 1D rotation would attenuate response to both the signal and the competing thermal noise. Hence, with a very good readout one can in principle overcome the attenuated response to the signal (readout electronics $1/f$ noise is also reduced at higher frequencies). However, in the presence of many orders of magnitude attenuation, it may be very hard to devise an adequate readout. As a general rule, reducing the response to the signal in a small force experiment is not a good strategy.

3. The ideas behind GG

GG is designed by the need to fulfill the following main drivers of a UFF/WEP experiment in space: (1) the test masses should be weakly coupled for high sensitivity (the weaker the better); (2) the apparatus should rotate in order to modulate the signal at high frequency (the higher the better); (3) the test masses should have high common-mode rejection (the higher the better) because the violation signal is differential while in space there is a large common-mode inertial force (mainly due to residual air drag on the spacecraft); (4) in low Earth orbit the two bodies of different composition should be concentric in order to reduce classical gravity gradient—or tidal—effects (the more concentric, the better).

As for driver 4 there is general agreement that the test bodies should be concentric coaxial cylinders. The question is: Should the symmetry axis of the cylinders lie in the orbit plane or should it be perpendicular to this plane? In the first case, the symmetry axis is the sensitive axis, i.e. the accelerometer is a 1D oscillator to be rotated around a non-symmetry axis. In the second case, the concentric cylinders form a 2D oscillator in the orbit plane rotating around the symmetry axis perpendicular to it. If the strategy is to actively control the test cylinders to prevent their motion and keep them concentric—in which case the signal is contained in the control force itself—then it is easier to control one direction only, and therefore, the natural

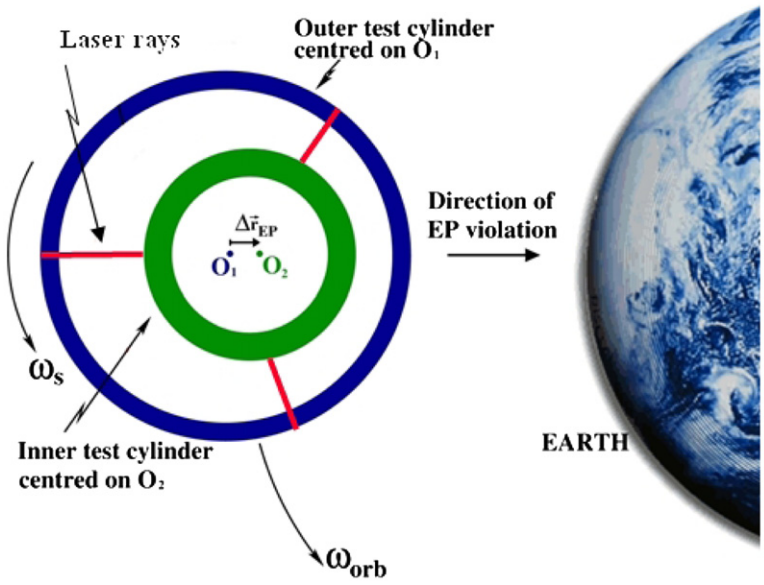

Figure 3. A section of the GG test cylinders in the plane of the orbit around the Earth at about 600 km altitude at the start of the mission with the symmetry/spin axes perpendicular to it (figure not to scale) is shown. Each cylinder spins around its symmetry axis at $\omega_s \simeq 2\pi$ rad s^{-1} while orbiting around the Earth at $\omega_{\rm GG} = 2\pi\nu_{\rm GG} = 2\pi\,1.7 \times 10^{-4}$ rad s^{-1}. A violation of the WEP would result in a differential displacement vector $\Delta\vec{r}_{\rm EP}$ pointing to the center of the Earth. For the GG target $\eta = 10^{-17}$ and a differential coupling frequency $\nu_d \simeq 1/540\,{\rm s}^{-1}$, it is $\Delta r_{\rm EP} = 8 \times 10^{-17}/(2\pi/540)^2 \simeq 0.6$ pm. The test cylinders, the weak mechanical joints which couple them and the laser gauge readout all corotate at $\omega_s \gg \omega_{\rm GG}$, thus up-converting and reading the signal at $\simeq \omega_s \simeq 2\pi$ rad s^{-1}.

choice is the first one (as in STEP [32] and μSCOPE[33]). From this choice, it follows that rotation perpendicularly to the symmetry axis must actively be provided.

However, each test mass forms a two-body problem with the Earth, and therefore, it has two degrees of freedom (in the orbital plane). UFF/WEP experiments are required to measure tiny relative deviations of the two masses from the same orbit that they should follow according to classical celestial mechanics. The test masses are very weakly suspended because if they were totally free, the experiment would be limited by release errors [34, 35], but in essence we deal with a two-body problem. If the masses are forced to move along one direction only (the sensitive axis) by making the suspensions very stiff in the other two directions, the cross coupling of such high stiffness with the sensitive axis while the masses tend to move in a plane is a serious issue [36, 37]. From a general physics viewpoint, it is much better to have a mechanical oscillator sensitive in the orbit plane too (as in GG) free to respond to external forces whose effect is measured by a good readout, auto-centering being ensured by physics laws.

In addition, the oscillator would rotate around its symmetry axis rather than perpendicularly to it; and by making the whole spacecraft cylindrically symmetric and co-rotating, it is possible to stabilize it passively simply by providing—at the start of the mission—the required spin frequency. Weak coupling of the spacecraft outer shell with the payload inside it provides the so-called nutation damping required for one-axis attitude stability.

Figure 3 shows a sketch of the GG test cylinders in the orbit plane around the Earth in the presence of a violation signal. In this configuration, disturbances along the cylinders'

axes, such as the radiometer effect, are not a limitation. In 1D sensors, the radiometer effect, caused by the residual gas in combination with temperature gradients across the axes of the cylinders, is a well-known differential systematic effect competing directly with the violation signal which sets severe requirements [38, 39].

Drivers 1 and 2 require very weak coupling and very fast spin, which is the definition of a mechanical oscillator rotating in the supercritical regime. As we have seen in section 2, this is possible in 2D (not in 1D), and it provides a very effective auto-centering of the test masses by physics laws and a highly reduced level of thermal noise due to internal damping, resulting in a very short integration time even for a UFF/WEP test to 10^{-17} at room temperature.

Drag on GG due to residual atmosphere along its orbit is 50 million times smaller than 1g, but it is also 2.5 billion times bigger than the target signal. Its effect is an inertial force on the suspended test masses which ideally should act the same on both of them (common-mode effect). In reality, it is not so; a good strategy is to partially compensate and partially reject it. A drag-free control system for GG has been developed in 2009 by TAS-I (Torino) based on GOCE expertise [40, chapter 7]. For the thruster technology, both FEEP and Cold Gas thrusters were considered. In 2011, a delta study was performed by TAS-I establishing Cold Gas thrusters as the baseline [41].

In order to reject common-mode forces (driver 3), we would like the cylinders to be coupled like in a balance. With mechanical suspensions this is possible, though not trivial. A very imaginative design was proposed by [42] (see [23, chapter 2, figure 2.7]) and updated in [40, chapter 3]: the concentric cylinders are arranged to form a peculiar beam balance with the beam along the cylinders axis made by appropriate coupling arms which can be adjusted with inch worm actuators in order to balance the balance. The whole design is perfectly symmetric w.r.t. the center of mass both in azimuth (cylindrical symmetry) and top/down. The common-mode force against which balancing is performed is the inertial force resulting from air drag on the spacecraft.

On ground against 1g beam balances are balanced to 5 parts in 10^{10} [43]. In GG, the force to be balanced is 50 million times smaller than 1g and the required level of balance (rejection of common-mode forces) is by 1 part in 10^5 [40, chapter 4]. The mechanical suspensions are very weak U-shape lamellae (a 10 kg proof mass inside GG requires a suspension that one would use on ground for suspending 0.2 mg against local gravity). They provide also passive electric discharging of the test masses, which is crucial in gravity experiments, but unlike dummy wires like those used to discharge the test bodies of μSCOPE, in GG they couple the masses in a well-designed manner and ensure a small value of the relevant losses (1/20 000).

After drag-free control, rejection of the remaining drag effect by the GG balance is very effective; hence, only a very small fraction produces a differential displacement of the test cylinders, while most of it acts the same on both of them. The readout must be insensitive to this common-mode effect; otherwise, it may be detected as differential—to some extent—and therefore compete with the signal. The great property of torsion balances on ground, whereby the center of mass is necessarily aligned with the fiber and common-mode forces are perfectly rejected, does not hold if the balance is at 0g. In space, we need *both* rejection of common-mode forces by the test masses *and* a differential readout.

The original GG readout was based on capacitance bridges, whose plates must be carefully centered halfway in between the test cylinders to ensure that its reading is not affected by their displacements in the common mode. A laser gauge interferometry readout developed and tested at Jet Propulsion Laboratory (JPL) with the noise level of $\simeq$ 1 pm Hz$^{-1/2}$ at 1 Hz will replace the capacitance bridges because it is less noisy and it ensures a better differential reading. In addition, it allows a larger gap between the cylinders (2 cm), making electric patch effects

negligible and reducing thermal noise due to gas damping. Last but not least, it deposits only light on the test cylinders. In order to measure the relative displacements of the test cylinders three laser gauges will be mounted at 120° from each other. The laser boxes will be located on the co-rotating intermediate stage (known as PGB) which encloses the test masses. Two layers of laser gauges, one above and one below the center of mass, will be used for full information on the relative motion of the test cylinders. In correspondence with each laser beam, the outer test cylinder will have a hole surrounded by a well polished reflective annular surface, and the inner test cylinder will have a small area also well polished and reflective. A similar system will be implemented on the ground prototype; 30 times higher noise level is acceptable in this case.

4. GG on ground: current sensitivity and target

GGG ('GG on Ground') is a 1g version of the 2D differential accelerometer to fly in GG. It is sensitive in the horizontal plane of the lab where the concentric coaxial test cylinders (10 kg each as in space) are weakly coupled while rotation occurs around the vertical/symmetry axis. The same 2D joints which couple the masses in the horizontal plane suspend them against local gravity. As a consequence, coupling cannot be as weak as in the absence of weight, which results in a reduced acceleration sensitivity as compared to the apparatus in space (by the ratio of the natural coupling frequencies squared). GGG is in essence a very peculiar beam balance—first proposed by [44] in 1996—with a vertical (rather than horizontal) beam and the masses concentric (rather than separated by the beam). These properties allow rotation around the (vertical) beam of the balance at frequencies higher than the natural one which couples the masses; thus the GGG dynamical system is in supercritical regime as required in space.

The essence of the GGG design is sketched in figure 4 and described in the caption. The differential period T_d of natural oscillation of the test bodies relative to each other can be written as

$$T_d^2 \simeq \frac{4\pi^2}{\frac{k_t+k_c+k_b}{2mL^2} - \frac{g}{2L}\frac{\Delta L}{L}}. \tag{3}$$

Here, m is the mass of each test body, g is the local gravitational acceleration, L is half the length of the balance coupling arm, $\Delta L/L$ is the level of unbalance of the balance, and k_t, $k_c$andk_b are the elastic constants in (Nm rad^{-1})—along each direction—of the 2D flexure joints sketched in the figure. The term depending on gravity in the denominator of (3) can be reduced by making $\Delta L/L$ sufficiently small, i.e. by sufficiently balancing the balance via adjustments of its arms length. In practice, in GGG, it is easier to adjust the masses of the balance rather than its arms; with 10 kg bodies, the required balancing depends on displacing sizable additional masses. The term depending on local gravity could in principle be used to obtain, with the same joints, a longer differential period (gravity would act as a negative spring) but this is in general non-convenient as far as tilts are concerned; one should also avoid the system to become unstable.

An additional 2D weak joint with elastic constant $k_{\rm shaft}$ has recently been mounted below the bearings on the rotating shaft with the purpose of passively reducing low frequency noise on the shaft due to terrain and bearings tilt and horizontal acceleration noise (figures 4(right) and 5(left)). The experimental results obtained with this system in supercritical rotation at $\simeq$ 0.2 Hz in a 29 d run are reported in figures 6 and 7 after demodulation to the non-rotating horizontal plane of the lab. During the run, the vacuum chamber is thermally stabilized; low frequency ambient temperature variations are reduced by two orders of magnitude.

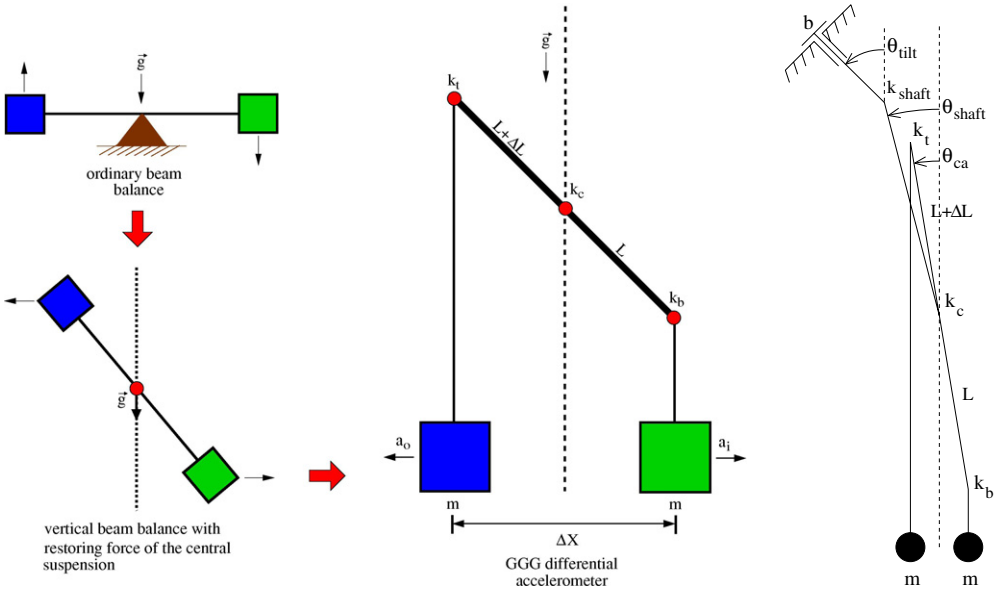

Figure 4. The GGG accelerometer is designed to be sensitive to differential forces acting in the horizontal plane of the lab while rotating in the vertical direction. (*left*) The two test masses depicted in blue and green are coupled by 2D weak joints to form a vertical beam balance. The coupling arm of the balance is shown (in black) with the 3 joints (in red). The central joint, of elastic constant k_c, sustains the whole weight and is the pivot center of the balance; the top and bottom joints, of elastic constants k_t and k_b, suspend the top and bottom mass respectively. The sketch refers to an unbalanced configuration of the balance in which the bottom half of the arm has length L while the top one is slightly longer, with length $L + \Delta L$. In this case the natural period of differential oscillation of the test masses T_d is given by (3). In the real GGG apparatus the masses are concentric coaxial *Al* cylinders weighing 10 kg each. (*right*): The upper part of the shaft, rotating on bearings b is tilted by the angle $\theta_{\rm tilt}$ due to terrain and bearings tilt noise. A 2D flexure joint $k_{\rm shaft}$ is placed on the shaft below the bearings. It suspends the balance of total mass $M_{\rm tot}$ with an arm of length $L_{\rm shaft}$ –from the joint $k_{\rm shaft}$ to the pivot center of the balance where the central joint k_c is located. At low frequencies, in response to an input tilt angle $\theta_{\rm tilt}$ the shaft is subject to a reduced tilt $\theta_{\rm shaft} = \frac{k_{\rm shaft}}{M_{\rm tot} g L_{\rm shaft}} \theta_{\rm tilt} \ll \theta_{\rm tilt}$. The corresponding equilibrium position of the coupling arm of the balance in response to the shaft tilt is $\theta_{ca} = \frac{k_c}{2mL^2} \frac{T_d^2}{4\pi^2} \theta_{\rm shaft}$. Note that low frequency horizontal acceleration disturbances are equivalent to tilt disturbances ($\Delta a_{\rm horiz-acc} = g\theta_{\rm tilt}$).

Figure 6 reports the time series of the relative displacements between the centers of mass of the test cylinders, showing that they remain close to each other within a few tens of nanometer for the entire duration of the run. As shown in figure 7(bottom), the relative displacement noise at the frequency 1.7×10^{-4} Hz relevant for the GG experiment in space is $\simeq$ 180 pm, which is 300 times larger than the target in space. Due to the current much stiffer coupling of the GGG test masses, the corresponding acceleration noise is $\simeq 7 \times 10^{-11}$ m s^{-2}, but we argue that there are no fundamental limitations to reducing it very significantly.

We state by the following arguments that GGG acceleration noise is currently limited by ball bearings tilt noise on the shaft. Input tilts $\theta_{\rm tilt}$ and the resulting differential acceleration $a_{\rm tilt}$ between the test cylinders are related (at low frequencies) by a simple analytical expression:

$$a_{\rm tilt} = \frac{k_c}{mgL} \frac{k_{\rm shaft}}{M_{\rm tot} g L_{\rm shaft}} g\theta_{\rm tilt}, \tag{4}$$

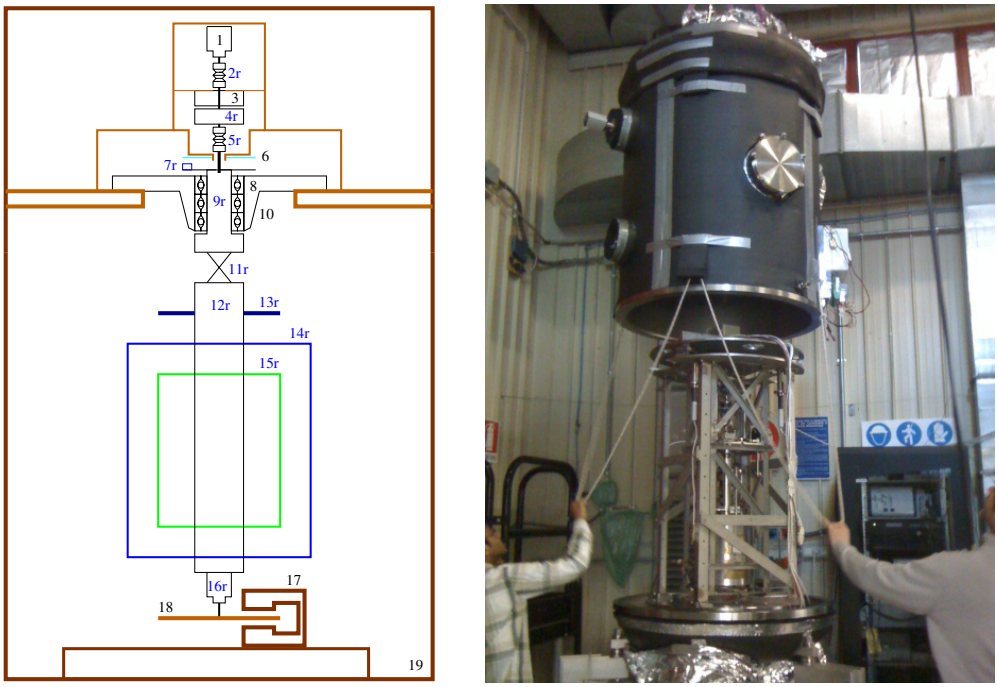

Figure 5. In order to isolate the GGG rotating accelerometer from low frequency terrain and ball bearings noise (tilts as well as horizontal accelerations), the current design (*left*) exploits the attenuation provided at low frequencies by the 2D flexible joint (labeled 11r—r refers to a rotating component) isolating the upper part of the shaft (9r)—which is subject to ground tilts and ball bearings (8) noise—from the lower part (12r), which holds the GGG balance. Thus, the isolated part of the shaft (12r) is driven by its weight closer to the direction of local gravity (which defines the vertical direction) more than its tilted top part. The picture to the right shows the experimental apparatus while opening the vacuum chamber.

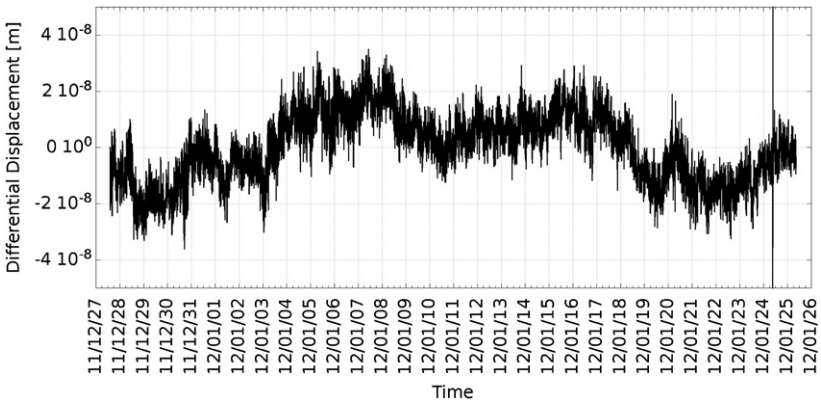

Figure 6. Time series of the relative displacements of the GGG test masses (frequencies above 1 mHz filtered out) in one direction of the horizontal plane of the lab during a 29 d run (stopped by the earthquake of 25 January 2012 with epicenter in Northern Italy).

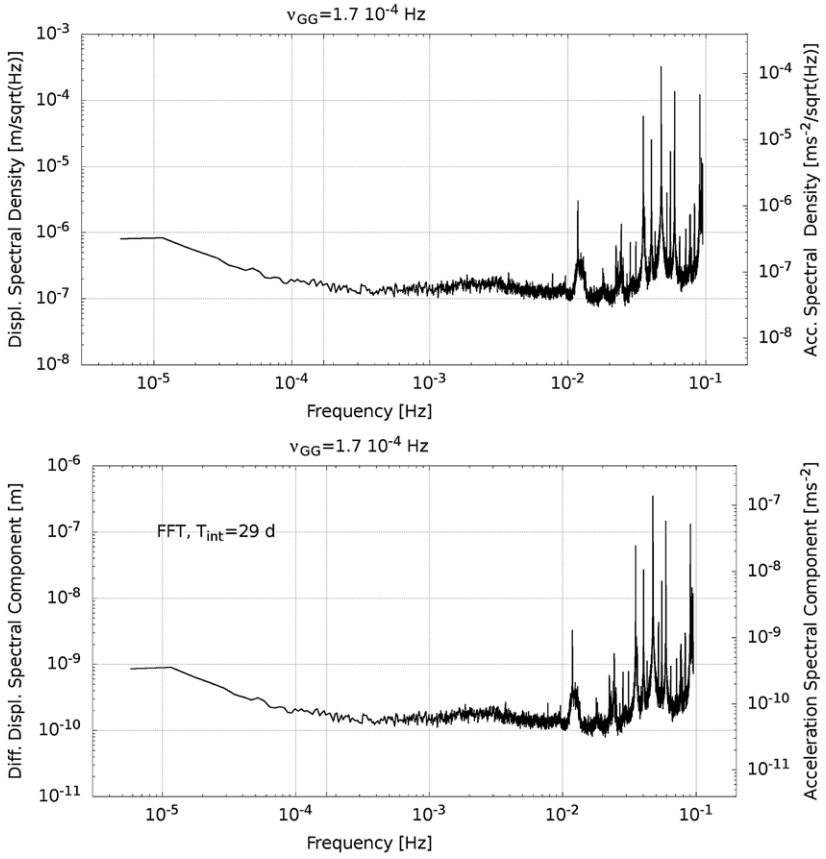

Figure 7. GGG noise performance as measured from a 29 d run. (Top) SD of the relative displacements and acceleration of the test cylinders in one direction of the horizontal plane of the lab; the GGG differential accelerometer is spinning at $\nu_{\rm spin} = 0.19$ Hz with the natural coupling frequency of 0.1 Hz. The measured relative displacement is $\simeq 1.8 \times 10^{-7}$m Hz$^{-1/2}$ and the measured relative acceleration is $\simeq 6 \times 10^{-8}$ m s^{-2} Hz$^{-1/2}$ at the frequency $\nu_{\rm GG} \simeq 1.7 \times 10^{-4}$ Hz, the orbital frequency relevant for GG in space. (Bottom) Measured relative test masses displacement and acceleration noise integrated over the full run duration. At $\nu_{\rm GG}$, we get an integrated differential displacement noise of $\simeq 1.8 \times 10^{-10}$ m and a differential acceleration noise of $\simeq 7 \times 10^{-11}$ m s^{-2}.

(see figure 4(right) for definition of the symbols) where all quantities except $\theta_{\rm tilt} = \theta_{\rm terrain} + \theta_{\rm ballbearing}$ are measured directly. Low frequency terrain tilts are not easy to measure; however, we rely on careful measurements carried out with various Italian Spring Accelerometer (ISA) instruments at IAPS lab (Roma Tor Vergata) [45] and at a former LABEN lab downtown Florence [46, chapter 7] to obtain a reliable estimate of the input tilt noise at the current INFN-GGG lab in San Piero a Grado, Pisa. With this estimate for $\theta_{\rm terrain}$, using (4) and the measured acceleration noise between the proof masses, we conclude that low frequency ball bearings noise is about two orders of magnitude bigger than terrain tilt noise (readout noise not being the limiting factor). From the ratio $a_{\rm tilt}/(g\theta_{\rm tilt})$, we also conclude that—at the frequency of interest—input tilt noise has been reduced by almost five orders of magnitude.

GGG acceleration noise due to input tilt noise can be further reduced by several orders of magnitude. In particular, low frequency tilt noise on the rotating shaft due to the bearings can be

Table 1. GGG goal and noise budget. The top part of the table shows the goal of GG in space and that of GGG on ground, with their relevant physical parameters. The bottom part of the table shows the error budget of GGG to reach its goal. We can see that terrain and bearings tilts and readout noise are the dominant noise sources, while thermal noise (from internal damping, residual gas and eddy currents) is lower. The relevant physical parameters used in the calculations are reported with the symbols as defined in section 4.

		GGG goal versus GG goal in space			
	Differential acceleration between test masses a at 1.7×10^{-4} Hz	a [ms^{-2}]	$r = a\frac{T_d^2}{4\pi^2}$ [m]	Integration time $T_{\rm int}$ [d]	
GG goal in space	$a_{\rm GG} = \eta g(h)$ (up-converted to 1 Hz)	8×10^{-17} ($\eta = 10^{-17}$, $h \simeq 600$ km)	6×10^{-13} ($T_d \simeq 540$ s)	1	
GGG goal	$a_{\rm GGG} = 10 a_{\rm GG}$ (up-converted to $0.2 \div 3$ Hz)	8×10^{-16}	3.2×10^{-14} ($T_d \simeq 40$ s)	30	
		GGG noise budget at 1.7×10^{-4} Hz			
Noise source	Δa [10^{-13} m s^{-2}Hz$^{-1/2}$]	Integrated Δa ($T_{\rm int} = 30$ d) [10^{-16}m s^{-2}]	Δr ($T_d \simeq 40$ s) [10^{-11}mHz$^{-1/2}$]	Integrated Δr ($T_{\rm int} = 30$ d) [10^{-14}m]	Conditions and physical data
Tilt noise sources: $a_{\rm tilt} = \frac{k_c}{mgL}\frac{k_{\rm shaft}}{M_{\rm tot}gL_{\rm shaft}} g\theta_{\rm tilt}$, $\theta_{\rm tilt} = \theta_{\rm terrain} + \theta_{\rm airbearing}$					
Terrain	8.2	5.1	3.3	2.1	$\theta_{\rm terrain} \simeq 8 \cdot 10^{-6}\ \frac{\rm rad}{\sqrt{\rm Hz}}$
Air bearing	4.1	2.5	1.7	1.0	$\theta_{\rm airbearing} \simeq 4 \cdot 10^{-6}\ \frac{\rm rad}{\sqrt{\rm Hz}}$
					$k_c \simeq k_{\rm shaft} \simeq 0.04$ Nm/rad
					$m = 10$ kg $L = 0.5$ m
					$M_{\rm tot} \simeq 80$ kg $L_{\rm shaft} \simeq 4$ m
Thermal noise sources [1, 25]					
Suspensions	1.3	0.8	0.5	0.3	$\phi = 1/20\,000$, $\nu_{\rm spin} = 0.2$ Hz
Eddy currents	1.3	0.8	0.5	0.3	no μmetal magnetic shield
Residual gas	0.5	0.3	0.2	0.1	2 cm gap, P $= 10^{-4}$ Pa
Readout noise: $a_{\rm ROnoise} = (4\pi^2/T_d^2) r_{\rm ROnoise}$					
Laser gauge	7.4	4.6	3.0	1.8	$T_d \simeq 40$ s
Total noise	12	7.4	4.8	3.0	

reduced below the local terrain tilt noise by using air bearings instead of ball bearings. Although we are using ceramic ball bearings, they are known to be several orders of magnitude more noisy than air bearings. For instance, the entire vacuum chamber enclosing the torsion balance of the Eöt-Wash experiments rotates on air bearings. In GGG, this would be unpractical; hence, we must solve the problem of a rotating shaft going from air to vacuum. Commercial solutions are available for this problem which can be adapted to the GGG case. Once bearings noise is smaller than local terrain tilt noise, various physical quantities in (4) can be optimized to further reduce the effect of terrain tilts on the test masses.

Although terrain tilt and bearings noise are absent in the space experiment (high rotation energy, spacecraft isolation, the absence of motor and bearings) on ground, this noise must be drastically reduced in order to demonstrate a performance close to that required in space. It is quite interesting that there appear to be no fundamental limitations to setting for GGG the task of measuring an acceleration noise only ten times larger than required for GG in space, namely $8 \times 10^{-16}\,\mathrm{m\,s^{-2}}$ at the GG orbital frequency (up-converted by rotation to $0.2 \div 3$ Hz). The error budget reported in table 1 shows that for a 30 d integration time thermal noise is not a limitation. However, several important improvements are required to reduce tilts and bearings noise, weaker suspensions and good balancing are needed to reach a longer differential period. A laser gauge readout similar to that planned for GG in space will be implemented with a noise level of 30 pm $\mathrm{Hz^{-1/2}}$ at the rotation frequency.

5. Conclusions

GG can test gravity for composition dependence four orders of magnitude better than to date while orbiting around the Earth on a low altitude sun-synchronous orbit. It will test the universality of free fall and the WEP in the field of the Earth to 1 part in 10^{17} by searching for a differential acceleration signal of $\simeq 8 \times 10^{-17}\,\mathrm{m\,s^{-2}}$ between proof masses of different composition. The signal (a 0.6 pm relative displacement of the masses) points to the center of mass of the Earth at the satellite orbital frequency 1.7×10^{-4} Hz and is up-converted to 1 Hz by its own rotation. The experiment is performed at room temperature because the relevant thermal noise is very low thanks to GG rapid rotation. Therefore, the integration time required to bring thermal noise below the signal and reach the mission goal is very short (a few hours). A low noise laser gauge readout developed and tested at JPL makes it possible to measure the target signal in such a short integration time. By allowing for about 15 satellite orbits (which take 1 day) to complete a single test, most of the mission duration time is available to establish with certainty the physical nature of the measurement by checking it against systematics. These checks rely on different dynamical conditions (of the sensor relative to the orbital plane) during the mission. They are performed with a single accelerometer located at the center of mass of the spacecraft; they are very robust and make additional accelerometers unnecessary.

An agreement exists between Agenzia Spaziale Italiana (ASI) and Jet Propulsion Laboratory (JPL) on submitting GG to the EXPLORER program of NASA as an American led mission with Italian partnership. EXPLORER is a very successful program dedicated to flying small size missions every few years; it has been highly ranked by the 2010 Decadal Astronomy Survey.

A very strong asset for GG is the GGG full scale prototype in the lab. On ground, the major error sources are terrain microseismic and bearings noise at low frequencies, both absent in space. We have recently designed and implemented on the rotating shaft a passive 2D joint for their attenuation and measured a relative displacement of $\simeq$180 pm, corresponding to a differential acceleration noise of $\simeq 7 \times 10^{-11}\,\mathrm{m\,s^{-2}}$ (at 1.7×10^{-4} Hz, up-converted by rotation

to $\simeq 0.2$ Hz). It is limited by ball bearings tilt noise. GGG error budget shows that along these lines, there are no fundamental limitations for the system to be substantially improved. Our target is to reach $\simeq 8 \times 10^{-16}$ m s^{-2} on ground (up-converted by rotation to $0.2 \div 3$ Hz). This would be only a factor 10 away from the sensitivity required in space for GG to meet its goal.

Acknowledgments

This work was supported by ASI and INFN and it was performed in part at JPL, Caltech, under a contract with NASA. The authors also thank the referees whose thorough analysis has helped in making the paper much better than it was when submitted.

References

[1] Pegna R *et al* 2011 *Phys. Rev. Lett.* **107** 200801
[2] Einstein A 1907 Relativitätsprinzip und die aus demselben gezogenen Folgerungen *Jahrbuch für Radioaktivität und Elektronik* **4** 411–62
Schwarz H M 1977 On the relativity principle and conclusions drawn from it Einstein's comprehensive 1907 essay on relativity: part III *Am. J. Phys.* **45** 899–902
[3] Dicke R H 1964 *The Theroretical Significance of Experimental Relativity* (London: Blackie)
[4] Will C M 2006 *Living Rev. Rel.* **9** 3 (http://relativity.livingreviews.org/Articles/lrr-2006-3/)
[5] Fuligni F and Iafolla V 1993 *Proc. STEP Symp. ESA WPP-115* p 104
[6] Bramanti D *et al* 1993 *Proc. STEP Symp. ESA WPP-115* p 319
[7] Etövös R V, Pekar D and Fekete E 1922 *Ann. Phys.* **68** 1166
[8] Einstein A 1916 Grundlage der allgemeinen relativitätstheorie *Ann. Phys.* **49** 769822
Einstein A 1952 The foundation of the general theory of relativity *The Principle of Relativity* (New York: Dover)
[9] Roll P G, Krotkov R and Dicke R H 1964 *Ann. Phys.* **26** 442517
[10] Braginsky V B and Panov V I 1972 *Sov. Phys.—JEPT* **34** 463-6
[11] Baeßler S *et al* 1999 *Phys. Rev. Lett.* **83** 3585
[12] Schlamminger S *et al* 2008 *Phys. Rev. Lett.* **100** 041101
[13] Williams J G, Turyshev S G and Boggs D H 2004 *Phys. Rev. Lett.* **93** 261101
[14] Mueller J, Hoffman F and Biskupek L 2012 Testing various facets of the equivalence principle with Lunar Laser Ranging *Class. Quantum Grav.* **29** 184006
[15] Adelberger E G *et al* 2009 *Prog. Part. Nucl. Phys.* **62** 102
[16] Murphy T W *et al* 2011 *Icarus* **211** 1103–8
[17] Nobili A M *et al* 2008 *Gen. Rel. Grav.* **40** 1533–54
[18] Peters A, Chung K Y and Chu S 1999 *Nature* **400** 949
[19] Fray S *et al* 2004 *Phys. Rev. Lett.* **93** 240–404
[20] Touboul P 2009 *Space Sci. Rev.* **148** 455-474
[21] Saulson P R 1990 *Phys. Rev.* D **42** 2437–45
[22] Touboul P 2011 *Rencontres de Moriond and GPhyS Colloqium 2011 Gravitational Waves and Experimental Gravity* slide 16 (http://moriond.in2p3.fr/J11/transparents/touboul.ppt)
[23] Nobili A M *et al* 1998 *GG Phase A Study Report ASI 1998* (http://eotvos.dm.unipi.it/ggweb/phaseA)
[24] Cagnoli G *et al* 1999 *Phys. Lett.* A **255** 230–5
[25] Pegna R *et al* Integration time in space experiments to test the equivalence principle (in preparation)
[26] Nobili A M *et al* Null checks of systematic errors in the GG space experiment to test the equivalence principle to 10^{-17} (in preparation)
[27] Nobili A M *et al* 1998 *New Astron.* **3** 175–218
[28] Den Hartog J P 1985 *Mechanical Vibrations* (New York: Dover) (first edition 1934)
[29] Nobili A M *et al* 1999 *Class. Quantum Grav.* **16** 1463–70
[30] Crandall S H 1970 *J. Sound Vib.* **11** 3–18
[31] Pegna R *et al* Upconverting low frequency signals above resonance (in preparation)
[32] Worden P W Jr 1976 *PhD Thesis* Stanford University, Stanford, CA, USA
[33] Touboul P, Foulon B and Le Clerc G M 1998 ONERA TP 1998–224 and IAF-98-B.3.07
[34] Blaser J P 2001 *Class. Quantum Grav.* **18** 2509
[35] Comandi G L *et al* 2003 *Phys. Lett.* A **318** 251–69
[36] Blaser J P 2000 On the motion of the STEP masses *STEP Note*

[37] Blaser J P 2001 Motion of a STEP mass with EP-violation *STEP Note*
[38] Nobili A M *et al* 2001 *Phys. Rev.* D **63** 101101
[39] Nobili A M *et al* 2002 *New Astron.* **7** 521–9
[40] Nobili A M *et al* 2009 *GG Phase A-2 Study Report ASI 2009* (http://eotvos.dm.unipi.it/PA2)
[41] Anselmi A 2011 private communication
[42] Bramanti D 1998 private communication
[43] Quinn T J, Speake C C and Davis R S 1986 *Metrologia* **23** 87–100
[44] Bramanti D 1996 private communication
[45] Iafolla V 2012 private communication
[46] Comandi G L 2004 *PhD Thesis* University of Pisa, Pisa, Italy